Mol. Cryst. Liq. Cryst., Vol. 527: pp. 80/[236]–91/[247], 2010

ISSN: 1542-1406 print/1563-5287 online
DOI: 10.1080/15421406.2010.486366

Taylor & Francis
Taylor & Francis Group

Study of Nematic Liquid Crystals by Spectroscopic Ellipsometry

VOLODYMYR TKACHENKO,[1]
ANTIGONE MARINO,[2] AND GIANCARLO ABBATE[2]

[1]CNR-SPIN Coherentia, Napoli, Italy
[2]CNR-SPIN and University of Naples Federico II, Napoli, Italy

We present an outline on the use of ellipsometry for nematic liquid crystals characterization. Possibility of anisotropic refractive indices measurement with accuracy up to 10^{-4} is demonstrated in the visible and near infrared wavelength ranges for different temperatures. Liquid crystal director distributions were measured both in cells with and without an applied voltage, subsequently the values of pretilt and polar anchoring strength were obtained by fitting the experimental data. Especial attention is paid to modifications of the commercial ellipsometer and to the choice of the proper data acquisition mode which improve the reliability and accuracy of measurements.

Keywords Anchoring energy; director distribution; liquid crystals; refractive index; spectroscopic ellipsometry

1. Introduction

Optical characterization of liquid crystals (LC), in a wide spectral range, is becoming a very important technical task because of their spreading applications in displays, optical telecommunication and other advanced areas of science and engineering. Because most of photonic applications of telecom interest fall in the wavelength region from 800 up to 1670 nm, the problem of obtaining LC refractive index measurements in the near infrared (NIR), with the same accuracy as in the visible – namely up to 10^{-4} – becomes topical.

Very precise optical techniques for characterization of LC, especially in NIR, are still not commercially developed, with the exception of the Variable Angle Spectroscopic Ellipsometry (VASE) [1]. Ellipsometry is based on measurements of the relative phase change Δ, and the relative amplitude change Ψ, for p- and s-polarization of the incident light, after transmission (or reflection) by the sample. Being generalized for anisotropic measurements it operates by additional parameters $\Psi_{ps,sp}$ and $\Delta_{ps,sp}$ which are linked to the off-diagonal elements of Jones matrices of a beam [1]. VASE technique can provide LC optical characterization in a very wide wavelength

Address correspondence to Volodymyr Tkachenko, CNR-SPIN Coherentia c/o Department of Physical Sciences, University of Naples Federico II, via Cintia M. S. Angelo 80126, Napoli, Italy. Tel.: +39-081676342; Fax: +39-081676342; E-mail: tkachenko@na.infn.it

range from near UV to near IR, covering display, telecom and most of the other photonic applications. In addition, the parameters characterizing surface anchoring can be obtained by VASE measurements with a surprisingly good accuracy.

Usual LC samples are sandwich cells, where the anisotropic film is confined between two thick glass plates, having additional layers on their inner surfaces. As a result of such multilayer structure, the ellipsometric measurements cannot be very sensitive to the refractive index of the thin internal layer of interest [2]. Moreover, the accuracy of the optical parameter values obtained by the experimental data inversion procedure depends dramatically both on the chosen physical model of the sample and on the initial guess for the parameters to be determined [3]. Thus, application of ellipsometry for LC study is not trivial.

In this article we present our developments of ellipsometry for studying nematic LC refractive indices and surface anchoring as well as some typical results recently obtained. All measurements were performed using the commercial ellipsometer VASE® from J.A.Woollam Co. Inc. To improve the reliability and accuracy of the sample characterization, we adapted VASE® for the Half Leaky Guided Mode (HLGM) technique. A sample holder was designed that can accommodate the high index glass prism on the sample upper side and a special software was used for analysis of the HLGM data. Taking into account strong temperature dependence of LC properties and to study that one, the sample holder was enclosed in a hot stage (from CaLCTec S.r.l.) allowing a sample temperature control within a wide range with accuracy of $\pm 0.1^{\circ}C$.

2. Optical Constants at Different Temperatures

We have integrated two standard optical techniques: VASE and HLGM spectroscopy, exploiting their best performances and overcoming their limits [4]. The integration of these techniques on the same VASE® hardware has the following advantages: 1) it overcomes the limitation to a small number of spectral lines of laser based HLGM set-ups and allows to perform continuous measurements in the whole spectral range from 270 to 1700 nm; 2) data acquisition is performed in the same experimental conditions and exploiting the same very precise software/hardware control of the VASE® instrument; 3) the two techniques are complementary, in the sense that each one is exploited to measure the LC parameters, to which it is more sensitive; 4) the combination of two spectrometric techniques increase the reliability and accuracy of the measurements with respect to the techniques considered individually.

HLGM spectroscopy requires that the LC film is sandwiched between two glasses: the upper glass with an index higher than the LC extraordinary index, and the bottom glass one lower than the LC ordinary one. Actually, for the upper and bottom substrates of the cell, we used SF6 and fused silica, respectively [4]. A beam impinges on the sample cell at variable angle through a prism optically matched to the upper glass by a suitable fluid (Fig. 1).

In this configuration, the LC film can be seen as a planar waveguide, whose TE and TM modes are guided at the interface with the bottom glass, but they are leaky at the interface with the upper glass, hence the name of the technique. The reflection coefficient is measured at the fixed wavelength in the angular range where the LC layer modes can be excited.

In the case of a planarly aligned cell, HGLM reaches the highest accuracy for p-p and s-s measurements and a proper choice of LC optical axis orientation. The

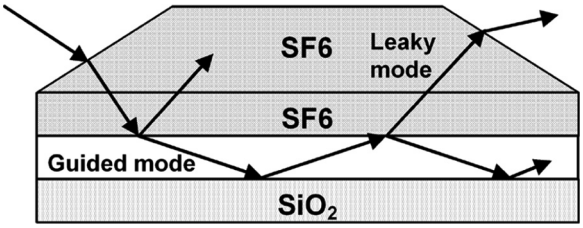

Figure 1. Scheme of a light propagating in the LC cell optically matched to the high index prism for HLGM measurements.

most suitable orientation of the optical axis is normal to the incidence plane, as the p- and s-polarized beams interact only with the LC ordinary n_o and extraordinary n_e refractive index, respectively, for every incidence angle. The actual sample may suffer imperfect adjustment and exhibit small film misalignment. A LC director inclination with respect to the normal to the incidence plane, out of and in the cell plane could then be present. These deviations from the assumed geometry result in different values of the effective index affecting the mode propagation constants.

The LC orientation parameters are determined by using spectroscopic ellipsometry, which is more sensitive than HLGM technique in this case. Transmission ellipsometry close to normal incidence is preferable because 1) it eliminates (or greatly reduces) unwanted incoherent reflections collected from the glass surfaces of the cell, 2) it isolates anisotropy measurements that are not affected by the presence of isotropic layers, nor by the absolute values of the LC refractive indices [5]. Because the LC samples are anisotropic and strongly depolarizing, both the generalized spectroscopic ellipsometry (g-SE) and the Mueller Matrix ellipsometry data are used [4–7].

The most important result that we achieve by integrating VASE and HLGM measurements is overcoming the accuracy limitation associated to these techniques using the results of each method as initial guess for the other method, in a feedback loop. In fact, our quoted refractive index values show the same accuracy level, namely 10^{-4}, in the whole spectral range [8], while previous measurements of the LC optical parameters were given with an accuracy lower in the NIR (not exceeding 10^{-3}) than in the visible.

Due to the absence of any resonances in the examined spectral range, we describe the ordinary and extraordinary indices of nematics by using the 3-parameter Cauchy formula:

$$n_{o,e} = A_{o,e} + B_{o,e}\lambda^{-2} + C_{o,e}\lambda^{-4} \tag{1}$$

The Cauchy parameters for the E7 and 5CB optical dispersion are presented in in Table 1 as obtained by fitting refractive index data for different wavelengths which are listed in Figure 2.

We applied the combined VASE-HLGM technique to measure the 5CB refractive indices at different wavelengths in visible and NIR spectral regions in a wide temperature range providing both the nematic and isotropic phases of LC. It is worth noting that ellipsometry measurements are not needed in isotropic phase because there is no preferable orientation of the LC molecules inside the cell. The results of

Table 1. Cauchy parameters for the E7 and 5CB optical dispersion at reduced temperature $T_c - T = 32 \pm 0.1\,K$ and $T_c - T = 5.8 \pm 0.1\,K$, respectively

LC	A_o	B_o (μm^2)	C_o (μm^4)	A_e	B_e (μm^2)	C_e (μm^4)
E7	1.49669	0.00785	0.00026	1.67906	0.01546	0.001663
5CB	1.50945	0.00934	0.00017	1.64499	0.01545	0.001019

5CB refractive index measurements for different temperatures and wavelengths are presented in Figure 2.

The four-parameter model for describing the temperature effect on the LC refractive indices has been recently proposed [9]:

$$\begin{aligned} n_o &= \alpha - \beta T - \frac{\Delta\nu}{3}\left(1 - \frac{T}{T_C}\right)^{\gamma} \\ n_e &= \alpha - \beta T + \frac{2\Delta\nu}{3}\left(1 - \frac{T}{T_C}\right)^{\gamma} \\ n_{mean} &= (n_e + 2n_o)/3 = \alpha - \beta T \end{aligned} \tag{2}$$

where parameters α and β can be obtained from fitting the temperature-dependent n_{mean} data at a given wavelength, and parameters $\Delta\nu$ and γ can be obtained by fitting the temperature-dependent $\Delta n = n_e - n_o$ data. Figure 3 shows the experimental 5CB refractive index dependence on temperature as well as approximation by the four-parameter model for $\lambda = 1550\,nm$.

Fitting the experimental data and the approximations by the four-parameter model we obtained the parameters of this model for each wavelength. Then we

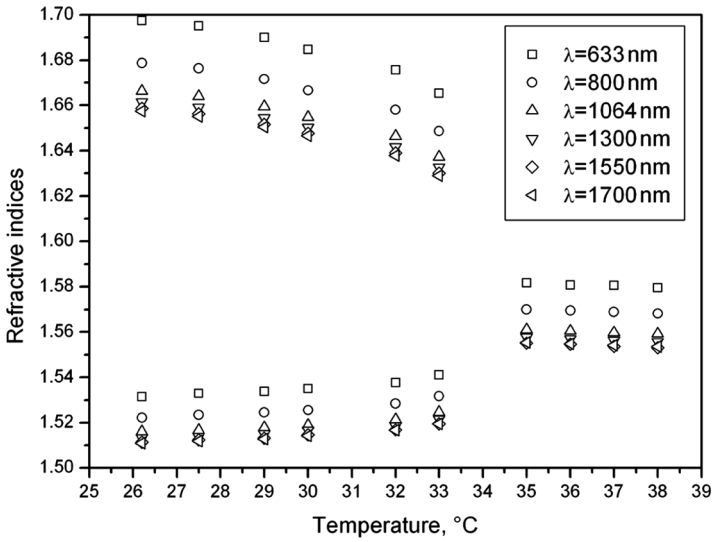

Figure 2. Temperature dependence of the 5CB refractive index in nematic and isotropic phases for six wavelengths.

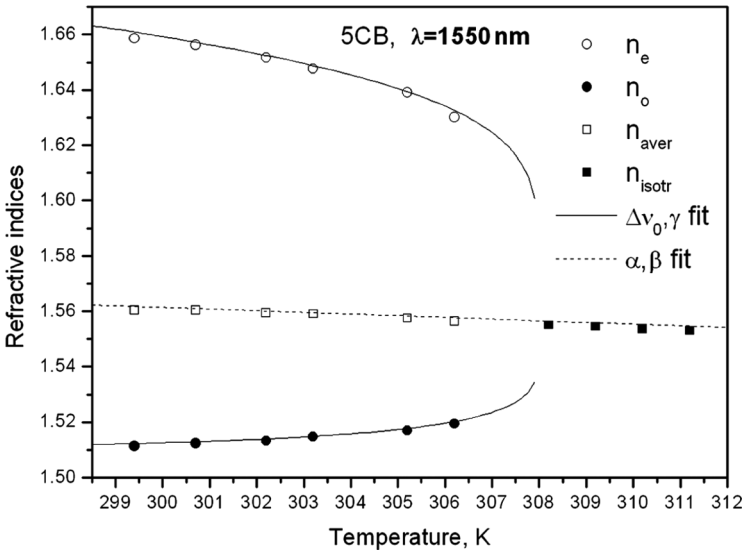

Figure 3. Experimental (points) and approximated by the four-parameter model (lines) temperature dependence of the 5CB refractive indices for $\lambda = 1550$ nm.

interpolate the dependences $\alpha(\lambda)$ and $\beta(\lambda)$ by polynomials: $\alpha = 1.85660 - 0.13746 \cdot \lambda + 0.03709 \cdot \lambda^2$ and $\beta = (0.73869 - 0.12780 \cdot \lambda + 0.01492 \cdot \lambda^2) \cdot 10^{-3}(\mathrm{K}^{-1})$. The dependence $\Delta\nu$ (λ) is approximated by Cauchy formula in accordance with LC dispersion low: $\Delta\nu = 0.27651 + 0.01247 \cdot \lambda^{-2} + 0.00174 \cdot \lambda^{-4}$. For the parameter γ we provide the value $\gamma = 0.1815$ as obtained by averaging over all wavelengths.

Using equations (2) and the obtained interpolation formulas for α, β, $\Delta\nu$, and γ refractive indices for any value of T and λ can be calculated with an error less than ± 0.001.

3. Pretilt and Anchoring Strength Measurements

Microscopic interaction between the anisotropic molecules of LC and those forming the surface is characterized by the anisotropic part of the surface free energy density F_S which depends on two parameters: the equilibrium position $\vec{n}_o$ of the LC director $\vec{n}$ along the easy axis of the substrate and anchoring strength W. In the approach of small deviation from the easy axis this dependence is described by the following formula proposed by Rapini and Papoular [10]:

$$F_s = -\frac{1}{2} W(\vec{n} \cdot \vec{n}_o)^2 \tag{3}$$

In the Vertical Aligned Nematic (VAN) cells, the easy axis is arranged almost perpendicular to the alignment layer, showing, in general, a small tilt angle with the normal to the sample plane, called pretilt.

The electro-optical properties of the VAN cell are strongly affected by the pretilt and anchoring strength. If the pretilt is null, the LC re-orientation direction upon electric switching is undefined, therefore the cell usually generates domains. Thus

a small pre-tilt is always needed for a proper device working. Higher pretilt leads to faster displays, because the time of electrical reorientation of LC molecules decreases. However, increasing the pretilt the quality of the dark state is reduced, because the birefringence in the off state increases accordingly.

The stronger anchoring in a VAN cell the shorter is the relaxation time when an electric field is switched off. On the other hand, the driving voltage increases with anchoring strength.

Thus a delicate balance between response time, contrast, and driving voltage has to be sought by optimizing pretilt and anchoring strength, possibly independently on each boundary surface of a VAN cell.

Optimization of the anchoring conditions implies the precise measurements of pretilt and anchoring strength in LC cells. Actually these measurements are related because to obtain W the known torque has to be applied to the LC molecules and the consequent tilt at the substrate has to be measured. Several techniques has been developed to measure these two quantities, however only the retardation [11–13] and Fully Leaky Guided Mode (FLGM) [14,15] ones are applicable to commercial-like cells. In both methods the tilt distribution across the whole LC layer is measured. The FLGM method is more reliable because it can determine the tilt profile unambiguously but it uses more complicated home-made apparatus.

We propose to apply ellipsometry for measurements both of pretilt and anchoring strength in the commercial-like LC cells using a commercial ellipsometer, adequate for a possible industrial implementation.

Cells were prepared with polished glass plates, pixels were imprinted on ITO coating by photolithography. Vertical alignment of LC was induced by thermal evaporation of SiO_x onto the glass plates. Different pretilt angles: 50°, 67°, 70°, and 80° were obtained by changing the thermal evaporation angle of the SiO_x. Coated substrates with antiparallel evaporation directions were assembled into sandwich cells with a gap of 4 μm filled with MLC6608 (Merck) nematic LC mixture, with negative dielectric anisotropy, $\Delta\varepsilon = -4.2$.

We adopt the following laboratory coordinates: the y-axis is normal to the incidence plane of the ellipsometer; the zenithal angle θ (tilt) is the one between the liquid crystal director and the z-axis; the azimuthal angle φ is the one between the y-axis and the director projection on the xy-plane. The sample was oriented with φ close to zero. We note that for the chosen orientation of the sample, the $\Psi_{ps,sp}$ and $\Delta_{ps,sp}$ parameters appear only for non-zero tilt, and grow with the angle of incidence. Thus this cell orientation provides particular sensitivity when the LC tilt distribution across the cell is measured.

The accuracy of the ellipsometry measurements depends on the adequacy of the optical model which has to take into account geometric, morphologic, and material properties of each layer of a multilayered sample under study. We used a 3-step strategy for measuring optical constants and thicknesses of the cell layers and LC tilt [16].

In the first step, spectroscopic reflection measurements were carried out from 400 nm up to 1700 nm (Fig. 4). Being particularly sensitive to refraction index variation, these data were used to obtain a first evaluation of the cell thickness L and ordinary and extraordinary indices of LC. Zero pretilt has been assumed at this stage. These measurements had been repeated for several incident angles of the impinging light to improve the accuracy of the results.

In the second step, transmission ellipsometric measurements were performed at a fixed wavelength (633 nm) versus the incident angle from −15 to 60 degree. In

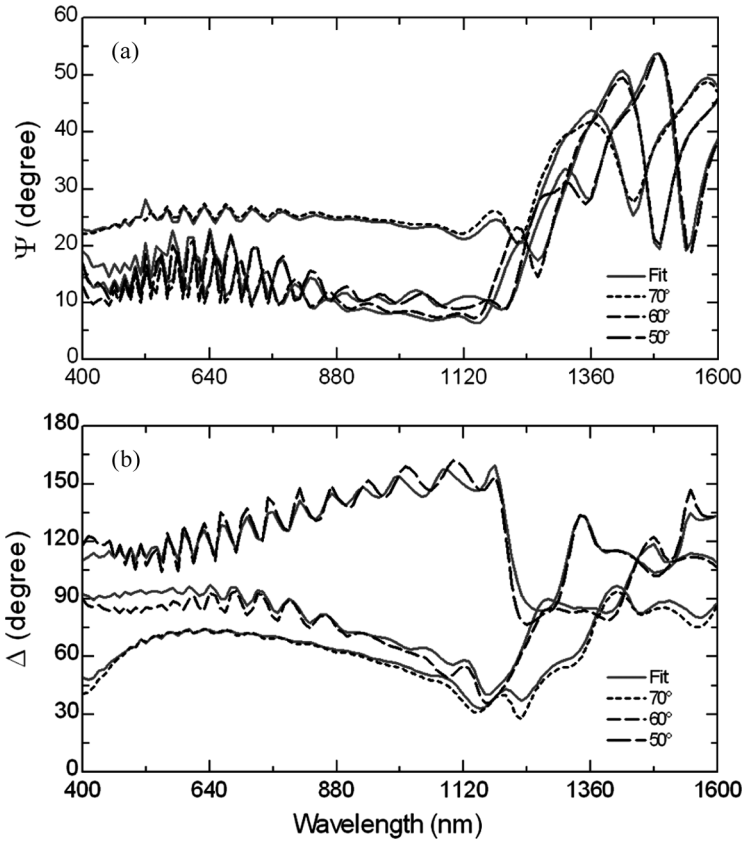

Figure 4. Ellipsometry spectra in reflection for the MLC6608 cell with SiO_x layers evaporated at 70° at both substrates: (a) – Ψ and (b) – Δ. Experimental (dashed lines) and fitted (full lines) curves are shown for three angle of light incidence: 50, 60, and 70°.

Figure 5, the Ψ, Δ, $\Psi_{ps,sp}$ and $\Delta_{ps,sp}$ parameters are presented according to the notation of VASE®:

$$\tan A_{nEt} \cdot \exp(i\Delta_{nEt}) = \frac{T_{pp}}{T_{ss}}, \quad \tan A_{spt} \cdot \exp(i\Delta_{spt}) = \frac{T_{sp}}{T_{ss}}, \quad \tan A_{pst} \cdot \exp(i\Delta_{pst}) = \frac{T_{ps}}{T_{pp}} \tag{4}$$

where T_{pp}, T_{ss}, T_{ps}, T_{sp} are the transmission Jones matrix elements. By the analysis of these data we obtained a first evaluation of the pretilt angles at the two surfaces, taking as fixed parameters the thicknesses and optical constants. The azimuthal angle φ was considered uniform across the cell, and its value was fitted to take into account the orientation of the LC director with respect to the laboratory coordinates.

In the third step, we analyzed reflection and transmission data together, keeping the previous values, obtained in steps 1 and 2, as starting point for a global fitting procedure that gave us the most accurate values for layer thicknesses, refractive indices, pretilt at the top and bottom surface of the LC cell.

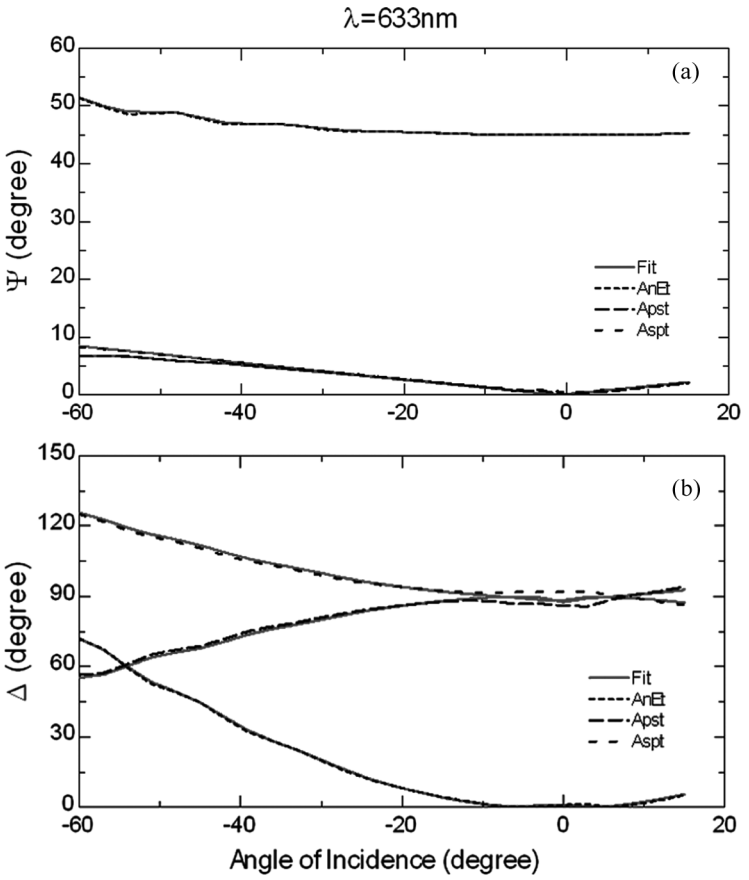

Figure 5. Experimental (dashed lines) and fitted (full lines) ellipsometry spectra in transmission for the MLC6608 cell with SiO_x layers evaporated at 70° at both substrates: (a) – Ψ and (b) – Δ. ($n_o = 1.475$, $n_e = 1.558$, $L = 3.65\,\mu m$, φ=0.8° as found by fitting both the reflection and transmission data).

A linear variation of the tilt angle was found in asymmetric cells due to the different pretilt on the two substrates. A smaller variation was found in symmetric cells as well. This is attributed to imperfections in the repeatability of the deposition process. Measurements were performed from both sides of the cell in order to double-check the reliability of results, showing, in all cases, inverted pretilt values for inverted positions of the cell.

Pretilt data averaged over different samples are plotted in Figure 6 for different angles of SiO_x evaporation.

To estimate anchoring strength, the LC director field is distorted by an external electric field and the consequent LC director distribution is determined by means of ellipsometry. As usually, an inversion data analysis must be performed building up an optical model that best describes the system. The LC director profile is simulated by the theory to be used in the optical model.

The LC tilt distribution $\theta(z)$ along the cell depth is obtained as a solution of the Euler-Lagrange equation, which minimizes the free energy of the LC inside the cell

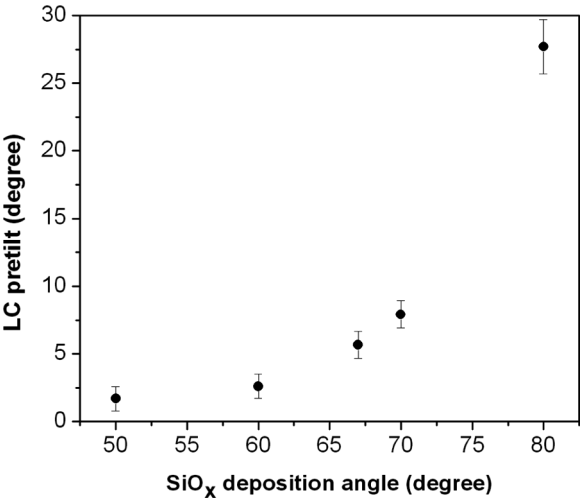

Figure 6. MLC6608 pretilt dependence on SiO_x evaporation angle.

under the action of an applied electric field:

$$(1 - k\sin^2\theta)\theta'' - k\sin\theta\cos\theta\cdot\theta'^2 + \frac{L^2(\varepsilon_\perp - \varepsilon_{//})D_z^2\sin\theta\cos\theta}{k_{33}\ \varepsilon_0\varepsilon_{//}^2(1 - u\sin^2\theta)^2} = 0, \tag{5}$$

where $k = 1 - \frac{k_{11}}{k_{33}}$; $u = \frac{\varepsilon_{//} - \varepsilon_\perp}{\varepsilon_{//}}$; k_{11} and k_{33} – the Frank elastic coefficients; $\varepsilon_{//}$ and $\varepsilon_\perp$– dielectric permittivity components of LC; L – the LC layer thickness. Electric displacement D_z is connected to voltage V applied to the cell by the formula:

$$V = \frac{D_z L}{\varepsilon_0\varepsilon_{//}}\left(\int_0^1 \frac{d\zeta}{1 - u\sin^2\theta(\zeta)} + \frac{2\varepsilon_{//}\,d_{AL}}{\varepsilon_{AL}L}\right), \tag{6}$$

where d_{AL} and ε_{AL} – are the thickness and dielectric constant of the alignment layer, respectively. The first and the second terms in the bracket correspond to voltages applied to the LC layer and to two alignment layers, respectively.

Boundary conditions at the LC-glass interfaces are taken in the Rapini and Papoular approach:

$$\begin{aligned}\left[k_{11}\sin^2\theta(0) + k_{33}\cos^2\theta(0)\right]\ \frac{d\theta}{dz}(0) &= W\sin[\theta(0) - \theta_0]\ \cos[\theta(0) - \theta_0]\\ \left[k_{11}\sin^2\theta(L) + k_{33}\cos^2\theta(L)\right]\ \frac{d\theta}{dz}(L) &= -W\sin[\theta(L) - \theta_L]\ \cos[\theta(L) - \theta_L]\end{aligned} \tag{7}$$

where θ_0 and θ_L are the pretilt values at the boundaries.

Using the simulated tilt profile achieved from Equations (5)–(7), we generated data curves of the ellipsometer parameters, Ψ and Δ. These are then compared with the experimental ones, in order to minimise the mean square error (MSE). During simulations the input values for all the relevant parameters, apart from the anchoring energy, were taken either from the literature (e.g., elastic and dielectric constants)

or from our measurements at zero field (e.g., refractive indices and pretilt) and kept constant. The anchoring energy was the only fitting parameter, letting the applied voltage as the external parameter. The searched W value was obtained in correspondence to the MSE minimum. Thus, an off-line fit has been performed for a number of voltages in a range from 0 to 3 V.

As an example, we report the result of W measurement for the cell with a SiO_x deposition angle of 50° on both substrates. In this case, the input parameters for the tilt profile simulation were: $\theta_0 = 0.9°$, $\theta_L = 4.6°$, $\varphi = 1.8°$, $L = 3.75\,\mu m$, $\varepsilon_{AL} = 3.9$, $d_{AL} = 18\,nm$. The LC physical properties are listed as follows: $k_{11} = 16.7pN$, $k_{33} = 18.1pN$, $\varepsilon_{//} = 3.6$, $\varepsilon_{\perp} = 7.8$ (all the data were measured at 25°C). In Figure 7, the simulated tilt profile is shown for three W values: the one corresponding to $W = 5 \cdot 10^{-4}\,J/m^2$, which approximately gives the minimum of MSE and two other differing for ±10%. The inset shows the near-surface tilt profile.

In spite of the fact that the three tilt curves reveal very small differences among each other, the integral effect of the tilt profile on the MSE value is quite distinguishable.

Let us recall that the WVASE32® considers the MSE as the critical parameter for deciding about the quality of the fit and the MSE is related to the commonly used statistic χ^2. Actually, in our case the χ^2 can be used more intuitively to obtain an estimate of the uncertainty in the fitted parameter [17]. Near the local minimum in any fitted parameter, the χ^2 is a quadratic function of that parameter. For each voltage the minimum of the parabola (χ^2_{min}) corresponds to the sought W value, while the abscissae, corresponding to $\chi^2_{min} + 1$, define the one standard deviation limits: $W - \sigma_W$ and $W + \sigma_W$. Here σ_W is the estimation provided by our fitting procedure of the standard error in W.

The results of W measurements are: 5.1 ± 0.3, 5.4 ± 0.1, and $5.6 \pm 0.1 \cdot 10^{-4}\,J/m^2$ for voltages of 2.0, 2.5, and 3.0 V, respectively. At the lowest voltage σ_W is twice than

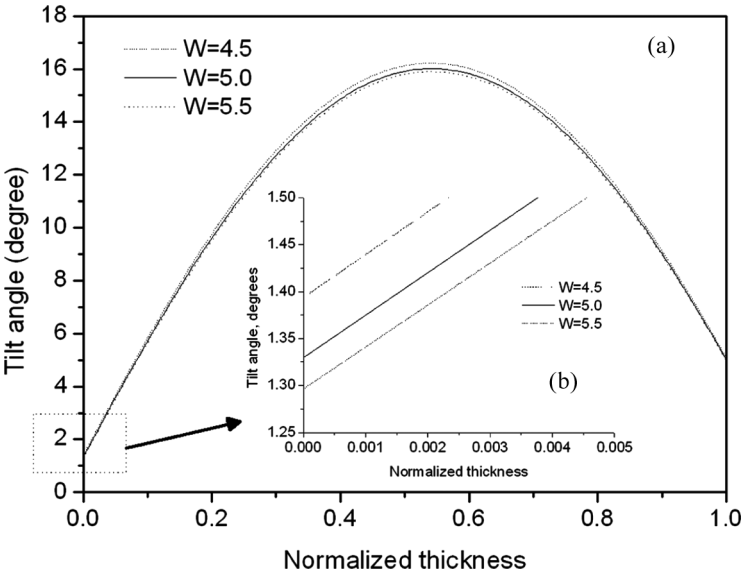

Figure 7. (a) Tilt profile at $V = 2\,V$ for three anchoring energy strengths. (b) in the inset, the near-surface pretilt changes due to different W ($10^{-4}\,J/m^2$) values are distinguishable.

the corresponding values at the higher voltages, where the larger LC director field distortion increases the sensitivity of the measuring technique. Hence, we provide the weighted mean, and the corresponding standard error, as the best estimate for the anchoring strength: $W = 5.5 \pm 0.07 \cdot 10^{-4}\,\mathrm{J/m^2}$.

It is worth noting that the overall W error depends on the uncertainties in all those parameters, namely pretilt, cell thickness, refractive indices, LC elastic constants, and components of dielectric permittivity tensor. Assuming there's no correlation between the parameters, we provide an estimation of the maximum overall error of 10%. This error estimation confirms that the present technique is among the most accurate for the evaluation of W.

4. Conclusions

We proposed the spectroscopic ellipsometry as a reference technique for liquid crystal characterization. The measure of the optical constants, their dependence from temperature, pretilt, tilt distribution, and anchoring strength in nematic LC cells can be carried out with a good accuracy.

A meaningful ellipsometric data inversion is strictly dependent on the choice of a proper physical model, and, above all, the final multi-parameter fitting procedure may critically depend on a good initial guess. That is why, to improve the reliability and accuracy of the optical constants measurements, we have integrated the variable angle spectroscopic ellipsometry with the half leaky guided mode spectroscopy.

Furthermore, to determine anchoring energy we developed a method based on a fitting procedure that combine experimental ellipsometric data and simulated theoretical results, having the anchoring strength as the only fitted parameter.

Ellipsometry can be applied to commercial-like cells for LC display application. Moreover, we used a commercial ellipsometer, adequate for a possible industrial implementation, allowing a standardization of measurements.

References

[1] Azzam, R. M. A., & Bashara, N. M. (1988). Ellipsometry and polarised light, North-Holland, Amsterdam, 1979; see also D. Y. K. Ko and J. R. Sambles, *J. Opt. Soc. Am.*, *A 5*, 1863.
[2] Aspnes, D. E. (2004). *Thin Solid Films*, *455–456*, 3.
[3] Tkachenko, V., Marino, A., Vita, F., D'Amore, F., De Stefano, L., Malinconico, M., Rippa, M., & Abbate, G. (2004). *Eur. Phys. J. E*, *14*, 185.
[4] Tkachenko, V., Abbate, G., Marino, A., Vita, F., Giocondo, M., Mazzulla, A., & De Stefano, L. (2006). *Appl. Phys. Lett.*, *89*, 221110.
[5] Hilfiker, J. N., Johs, B., Herzinger, C. M., Elman, J. F., Montbach, E., Bryant, D., & Bos, P. S. (2004). *Thin Solid Films*, *455–456*, 596.
[6] Hilfiker, J. N., Herzinger, C. M., Wagner, T., Marino, A., Delgais, G., & Abbate, G. (2004). *Thin Solid Films*, *455*, 591–595.
[7] Tkachenko, V., Abbate, G., Marino, A., Vita, F., Giocondo, M., Mazzulla, A., & De Stefano, L. (2006). *Mol. Cryst and Liq. Cryst.*, *454*, 271–279.
[8] Abbate, G., Tkachenko, V., Marino, A., Vita, F., Giocondo, M., Mazzulla, A., & De Stefano, L. (2007). *Journal of Applied Physics*, *101*, 073105.
[9] Li, J., Gauza, S., & Wu, S.-T. (2004). *Journal of Applied Physics*, *19*, 96.
[10] Rapini, A., & Papoular, M. (1969). *J. Phys. Colloques*, *30*, C4–54.
[11] Rosenblatt, C. (1984). *J. Phys.(Paris)*, *45*, 1087.

[12] Yokoyama, H., & van Sprang, H. A. (1985). *J. Appl. Phys.*, *57*, 4520.
[13] Nastishin, Yu. A., Polak, R. D., Shiyanovskii, S. V., Bodnar, V. H., & Lavrentovich, O. D. (1999). *J. Appl. Phys.*, *86*, 4199.
[14] Yang, F., Sambles, J. R., Don, Y., & Gao, H. (2000). *J. Appl. Phys.*, *87*, 2726.
[15] Yang, F., Ruan, L., & Sambles, J. R. (2000). *J. Appl. Phys.*, *88*, 6175.
[16] Marino, A., Santamato, E., Abbate, G., Tkachenko, V., Bennis, N., Quintana, X., & Otón, J. M. (2009). *Appl. Phys. Lett.*, *94*, 013508.
[17] Bevington, P. R., & Robinson, D. K. (2003). *Data Reduction and Error Analysis for the Physical Sciences,* 3rd Ed., McGraw-Hill Higher Education: New York.